Mathematical Properties of Objective Eulerian Coherent Structures and New Method for Visualization

Peter J. Nolan, Shane D. Ross

Contents

1 Introduction

Lagrangian analysis using techniques such as the finite-time Lyapunov exponent (FTLE) field or Lagrangian coherent structures can be very informative as to the dynamics of a system, however these methods can be time consuming to integrate and tricky to interpret. Recent developments in dynamical systems theory have generated new Eulerian methods, such as objective Eulerian coherent structures (OECS), for the anaylsis of dynamical systems. In this paper we will build upon this previous work by connecting OECS to FTLE, and providing a new method for the visualization of OECS.

2 Setup and Notation

The dynamical system

$$\frac{d}{dt}\mathbf{x}(t) = \mathbf{v}(\mathbf{x}(t), t), \tag{1}$$

$$\mathbf{x}_0 = \mathbf{x}(t_0). \tag{2}$$

Is often analyzed using Lagrangian methods, using the flow map for some time period of interest, $[t_0, t]$ given by,

$$\mathbf{F}_{t_0}^{t}(\mathbf{x}_0) = \mathbf{x}_0 + \int_{t_0}^{t} \mathbf{v}(\mathbf{x}(t), t)\, dt. \tag{3}$$

Mathematically rigorous methods such as LCS then involve Taking the gradient of the flow map we can then calculate the right Cauchy-Green strain tensor for the time period of interest,

$$\mathbf{C}_{t_0}^{t}(\mathbf{x}_0) = \nabla \mathbf{F}_{t_0}^{t}(\mathbf{x}_0)^T \cdot \nabla \mathbf{F}_{t_0}^{t}(\mathbf{x}_0), \tag{4}$$

The eigenvalues of which are

$$\lambda_1 < \lambda_2 < ... < \lambda_n \tag{5}$$

and are associated with the eignevectors

$$\boldsymbol{\xi}_{\lambda_i} \quad i \in \{1, \ldots, n\} \tag{6}$$

From the maximum eigenvalue of the Cauchy-Green tensor we get the FTLE

$$\sigma_{t_0}^{t}(\mathbf{x}_0) = \frac{1}{2|T|} \log(\lambda_n) \tag{7}$$

where $T = t - t_0$ is the (signed) elapsed time, often called the integration time.

The Eulerian strain tensor is defined as

$$\mathbf{S}(\mathbf{x}, t) = \tfrac{1}{2}\Big(\nabla \mathbf{v}(\mathbf{x}, t) + \nabla \mathbf{v}(\mathbf{x}, t)^T\Big) \tag{8}$$

The eigenvalues of which are

$$s_1 < s_2 < ... < s_n \tag{9}$$

and are associated with the eigenvectors

$$\boldsymbol{\xi}_{s_i} \quad i \in \{1, \ldots, n\} \tag{10}$$

Using the eigenvalues of the Eulerian strain tensor is a new method for the analysis of fluid flows. The minimum eigenvalue, s_1 was shown in ref [6] to provide a measure of instantaneous hyperbolic attraction, with minima of s_1 providing the cores of attracting objective Eulerian coherent structures.

3 Eigenvalues of S as FTLE limit for $n = 2$

For small $|T|$, we Taylor expand $\mathbf{C}_{t_0}^t(\mathbf{x})$ as

$$\mathbf{C}_{t_0}^t(\mathbf{x}) = \mathbb{1} + 2T\mathbf{S}(\mathbf{x}, t_0) + T^2\Big(\dot{\mathbf{S}}(\mathbf{x}, t_0) + \tfrac{1}{2}\nabla\mathbf{v}(\mathbf{x}, t_0)^T \cdot \nabla\mathbf{v}(\mathbf{x}, t_0)\Big) + \mathcal{O}(|T|^3) \quad (11)$$

where $\mathbb{1}$ is the $n \times n$ identity.

In what follows, we limit ourselves to the case $n = 2$. We note the following general result for the 2 eigenvalues, $\lambda^{\pm}(\mathbf{A})$, of 2×2 matrices $\mathbf{A}$ and scalar $\varepsilon \neq 0$,

$$\lambda^{\pm}(\mathbb{1} + \varepsilon\mathbf{A}) = 1 + \lambda^{\pm}(\varepsilon\mathbf{A}) \quad (12)$$

where

$$\lambda^{\pm}(\varepsilon\mathbf{A}) = \begin{cases} \varepsilon\lambda^{\pm}(\mathbf{A}), & \text{for } \varepsilon > 0 \\ \varepsilon\lambda^{\mp}(\mathbf{A}), & \text{for } \varepsilon < 0 \end{cases} \quad (13)$$

In (7), $\lambda_2 = \lambda^+(\mathbf{C}_{t_0}^t(\mathbf{x}))$. For small $T > 0$, we have

$$\lambda^+(\mathbf{C}_{t_0}^t(\mathbf{x})) = 1 + 2T\lambda^+(\mathbf{S}(\mathbf{x}, t_0)) + \mathcal{O}(T^2) \quad (14)$$

Thus,

$$\log(\lambda_2) = \log(1 + 2T\lambda^+(\mathbf{S}(\mathbf{x}, t_0))) = 2T\lambda^+(\mathbf{S}(\mathbf{x}, t_0)) = 2Ts_2(\mathbf{x}, t_0) \quad (15)$$

in the limit of small T using the Taylor expansion $\log(1 + \varepsilon) = \varepsilon$.

From (7), and noting that $|T| = T$ for $T > 0$, we have,

$$\sigma_{t_0}^t(\mathbf{x}) = \frac{1}{2|T|}\log(\lambda_2) = \frac{1}{2T}2Ts_2(\mathbf{x}, t_0) = s_2(\mathbf{x}, t_0) \quad (16)$$

Therefore, the largest eigenvalue of $\mathbf{S}(\mathbf{x}, t_0)$ is the limit of the FTLE value for forward time as $T \to 0^+$.

For $T < 0$ with small T, we have

$$\lambda^+(\mathbf{C}_{t_0}^t(\mathbf{x})) = 1 + 2T\lambda^-(\mathbf{S}(\mathbf{x}, t_0)) + \mathcal{O}(T^2) \quad (17)$$

Thus,

$$\log(\lambda_2) = 2T\lambda^-(\mathbf{S}(\mathbf{x}, t_0)) = 2Ts_1(\mathbf{x}, t_0) \quad (18)$$

From (7), and noting that $|T| = -T$ for $T < 0$, we have,

$$\sigma_{t_0}^t(\mathbf{x}) = \frac{1}{2|T|}\log(\lambda_2) = -\frac{1}{2T}2Ts_1(\mathbf{x}, t_0) = -s_1(\mathbf{x}, t_0) \quad (19)$$

Therefore, the negative of the smallest eigenvalue of $\mathbf{S}(\mathbf{x}, t_0)$ is the limit of the FTLE value for backward time as $T \to 0^-$.

If we denote s_1 and s_2 as s^- and s^+, respectively, we can summarize the above result as

$$\sigma_{t_0}^t(\mathbf{x}) = \pm s^{\pm}(\mathbf{x}, t_0) \quad \text{as} \quad T \to 0^{\pm} \quad (20)$$

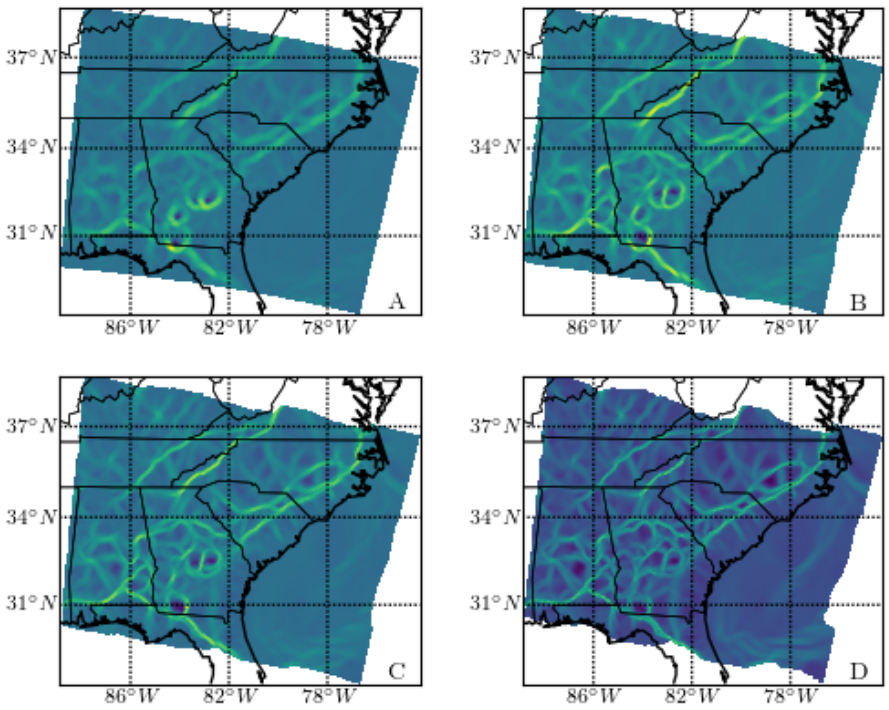

Figure 1: Comparison of s_1 to FTLE fields for different integration times. A) s_1 field, B) FTLE field T = −1 hr, C) FTLE field T = −2 hr, B) FTLE field T = −4 hrs.

4 S-Ridges as OECS

Previous work [1–5, 7–9] has demonstrated that LCS can be identified as Ridges of the FTLE field. Since s_1 and s_2 are the limits of the backward and forward time FTLE fields we propose to seek hyperbolic OECS as troughs of s_1 and ridges of s_2. This is in contrast to the definition proposed in [6] which focuses on saddle-type hyperbolic OECS as $\boldsymbol{\xi}_2$ and $\boldsymbol{\xi}_1$ tensor lines emanating from isolated minima and maxima of s_1 and s_2 respectively. This new definition expands the definition of OECS by looking at a broader class of attracting and repelling structures beyond saddle-type features.

In particular we propose OECS a new type of ridge we call an S-Ridge. S-Ridges are the limit of C-Ridges as integration time goes to 0. C-Ridges of the FTLE field have been proven to be mathematically equivalent to LCS. S ridges / troughs are material lines in the fluid flow which are locally orthogonal to the direction of maximal stretching. Since the direction of stretching is given by the eigenvectors of the Eulerian strain tensor, S, they are material lines who's gradient is locally orthogonal to the fields associated eigenvalue.

Mathematically we define attracting hyperbolic OECS as a trough line of the minimum eigenvalue field of $\mathbf{S}$, s_1.

$$s_1 < 0 \tag{21}$$
$$\nabla s_1 \cdot \boldsymbol{\xi}_1 = 0 \tag{22}$$
$$(\mathbf{H}_{s_1} \cdot \boldsymbol{\xi}_1) \cdot \boldsymbol{\xi}_1 > 0 \tag{23}$$
$$\tag{24}$$

further define repelling hyperbolic OECS as a ridge-line of the maximum eigenvalue field of $\mathbf{S}$, s_n.

$$s_2 > 0 \tag{25}$$
$$\nabla s_2 \cdot \boldsymbol{\xi}_2 = 0 \tag{26}$$
$$(\mathbf{H}_{s_2} \cdot \boldsymbol{\xi}_2) \cdot \boldsymbol{\xi}_2 < 0 \tag{27}$$
$$\tag{28}$$

These definitions, are mathematically consistent with the previous definition of a hyperbolic OECS, however, they form superset of the previous definition, as we are no longer reliant of isolated minima.

5 Real World Examples

For a real world demonstration we look at a WRF simulation over the South Eastern United States.

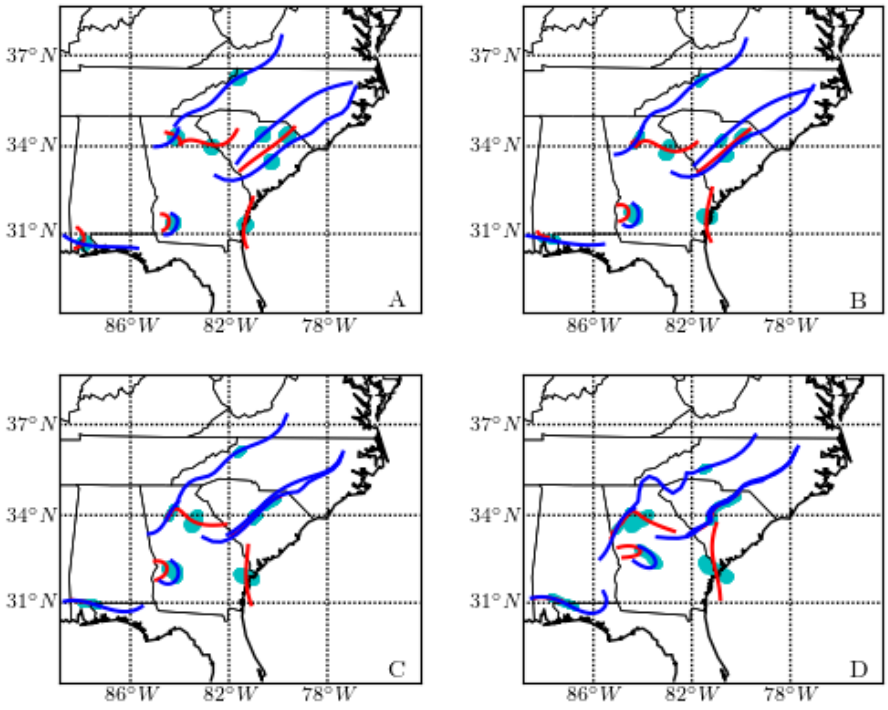

Figure 2: Comparison of s_1 to FTLE fields for different integration times. A) T=0, B) T=2hrs, C) T=4 hrs, B) T=8 hrs.

6 Extension to Higher Dimensions

We conjecture that it is possible to extend hyperbolic OECS to higher dimensions using the definitions, by exchanging s_2 and $\boldsymbol{\xi}_2$ for s_n and $\boldsymbol{\xi}_n$, where n is the dimension of the system being examined.

$$s_n > 0 \tag{29}$$
$$\nabla s_n \cdot \boldsymbol{\xi}_n = 0 \tag{30}$$
$$(\mathbf{H}_{s_n} \cdot \boldsymbol{\xi}_n) \cdot \boldsymbol{\xi}_n < 0 \tag{31}$$
$$\tag{32}$$

As an example we analyze the ABC flow. A simulation of intertial particles around an OECS in 3D can be found at, `https://youtu.be/fmXFcpUEfaI`

7 Conclusion

We conclude that for flows with spatial complexity of real world flows.

Future work will look for indicators of how the fields related to S change in time, better determining the extent of the time period over which OECS can be expected to give accurate predictions, and extending the proof of the FTLE field to higher dimensions.

8 Appendix

8.1 Proof of Eq. (12)

Let

$$\mathbf{A} = \begin{bmatrix} a & b \\ c & d \end{bmatrix}, \tag{33}$$

where $a, b, c, d \in \mathbb{R}$, then the eigenvalues of $\mathbf{A}$ are,

$$\lambda^{\pm}(\mathbf{A}) = \tfrac{1}{2}(a+d) \pm \tfrac{1}{2}\sqrt{(a+d)^2 - 4(ad-bc)}. \tag{34}$$

Now for $\mathbb{1} + \mathbf{A}$,

$$\mathbb{1} + \mathbf{A} = \begin{bmatrix} 1+a & b \\ c & 1+d \end{bmatrix}, \tag{35}$$

the eigenvalues are,

$$\begin{aligned}
\lambda^{\pm}(\mathbb{1} + \mathbf{A}) &= 1 + \tfrac{1}{2}(a+d) \pm \tfrac{1}{2}\sqrt{(2+a+d)^2 - 4(ad-bc+1+a+d)} && (36)\\
&= 1 + \tfrac{1}{2}(a+d) \pm \tfrac{1}{2}\sqrt{4 + 4(a+d) + (a+d)^2 - 4 - 4(a+d) - 4(ad-bc)} && (37)\\
&= 1 + \tfrac{1}{2}(a+d) \pm \tfrac{1}{2}\sqrt{(a+d)^2 - 4(ad-bc)} && (38)\\
&= 1 + \lambda^{\pm}(\mathbf{A}) && (39)
\end{aligned}$$

References

[1] A. E. BozorgMagham and S. D. Ross, *Atmospheric lagrangian coherent structures considering unresolved turbulence and forecast uncertainty*, Communications in Nonlinear Science and Numerical Simulation, 22 (2015), pp. 964–979.

[2] A. E. BozorgMagham, S. D. Ross, and D. G. Schmale III, *Real-time prediction of atmospheric lagrangian coherent structures based on forecast data: An application and error analysis*, Physica D: Nonlinear Phenomena, 258 (2013), pp. 47–60.

[3] A. E. BozorgMagham, S. D. Ross, and D. G. Schmale III, *Local finite-time lyapunov exponent, local sampling and probabilistic source and destination regions*, Nonlinear Processes in Geophysics, 22 (2015), pp. 663–677.

[4] B. Schindler, R. Peikert, R. Fuchs, and H. Theisel, *Ridge concepts for the visualization of lagrangian coherent structures*, Topological Methods in Data Analysis and Visualization II, (2012), pp. 221–235.

[5] C. Senatore and S. D. Ross, *Detection and characterization of transport barriers in complex flows via ridge extraction of the finite time lyapunov exponent field*, International Journal for Numerical Methods in Engineering, 86 (2011), pp. 1163–1174.

[6] M. Serra and G. Haller, *Objective eulerian coherent structures*, Chaos: An Interdisciplinary Journal of Nonlinear Science, 26 (2016), p. 053110.

[7] S. C. Shadden, F. Lekien, and J. E. Marsden, *Definition and properties of lagrangian coherent structures from finite-time lyapunov exponents in two-dimensional aperiodic flows*, Physica D: Nonlinear Phenomena, 212 (2005), pp. 271–304.

[8] P. Tallapragada and S. D. Ross, *A set oriented definition of finite-time lyapunov exponents and coherent sets*, Communications in Nonlinear Science and Numerical Simulation, 18 (2013), pp. 1106–1126.

[9] P. Tallapragada, S. D. Ross, and D. G. Schmale, *Lagrangian coherent structures are associated with fluctuations in airborne microbial populations*, Chaos, 21 (2011), p. 033122.